Available online at www.sciencedirect.com
ScienceDirect
Journal of Sound and Vibration 300 (2007) 863–876
JOURNAL OF SOUND AND VIBRATION
www.elsevier.com/locate/jsvi

Crack identification in a stepped beam carrying a rigid disk

Samer Masoud Al-Said[1]

Mechanical Engineering Department, Jordan University of Science and Technology, Irbid, Jordan

Received 20 May 2005; received in revised form 19 April 2006; accepted 8 September 2006
Available online 7 November 2006

Abstract

In this study, a simple algorithm based on a mathematical model is proposed to identify crack location and depth in a stepped cantilever Euler–Bernoulli beam carrying a rigid disk at its tip. The mathematical model that describes the lateral vibration of the beam is derived using the assumed mode method that coalesces with the Lagrange's equation. A massless torsional spring whose stiffness depend on the severity of the crack is used as a crack model. Using this crack modeling method combined with the assumed mode method, the crack effect is introduced to the system flexibility as global additional structural flexibility. For the assumed mode method, the mode shapes for two uniform beams connected by a massless torsional spring (simulating the cracked beam) are adopted as trial functions. The proposed identification algorithm utilizes the first three natural frequencies shift of the beam caused by a crack to estimate its location and depth. In addition, the proposed mathematical model is used to illustrate the effect of the crack depth and its location on the dynamic characteristics of the system. Using the commercial finite element (FE) software (ANSYS 8.0), three-dimensional finite element analysis (FEA) is carried out to show the accuracy of the derived mathematical model and to demonstrate the reliability of the proposed crack identification algorithm. The analysis showed consistency with the assumed mode results. It showed that the error in concurrent prediction of crack depth and its location using the proposed algorithm is about 10%.

1. Introduction

Mechanical accidents, fatigue, erosion, corrosion, as well as environmental attacks, are issues that can lead to a crack in a mechanical structure. Cracks are indications of an impending mechanical failure. In view of the fact that the presence of a crack in a structure could lead to devastating results, investigating the structural integrity of machines was an extremely active area of research in the last two decades. Although the theory and technology of non-destructive testing is highly enhanced, inspecting the integrity of a structure is a labor-intensive and protracted process that should only be carried out when it is truly needed. One tactic for reducing inspection-related shutdown time and cost is to furnish a mechanism with an early warning failure device. Such a device monitors, online, crack-related abnormalities in the behavior of a system. If the device gives a warning signal that a crack is present, an advisory message is given out to the operator to shutdown the machine and have it inspected. For the development of such early warning devices, awareness of the dynamics

E-mail address: masoud@just.edu.jo.
[1]Currently visiting associate professor at King Saud University, Riyadh, Kingdom of Saudi Arabia.

0022-460X/$ - see front matter
doi:10.1016/j.jsv.2006.09.011

Nomenclature

a	crack depth
B	beam width
D	crack depth ratio (a/H_c)
E	modulus of elasticity
H_1	half beam height at thick section
H_2	half beam height at thin section
H_c	half beam height at crack location
H_{12}	non-dimensional parameter H_1/H_2
H_{c2}	non-dimensional parameter H_c/H_2
H_{2L}	non-dimensional parameter H_2/L_b
I	beam cross section area moment of inertia about Z-axis
J	beam mass moment of inertia per unit length about Z-axis $J = \rho I$
J_d	disk mass moment of inertia about Z-axis $J_d = M_d R_d^2$
$\mathbf{K}$	modal stiffness matrix for intact beam of $N \times N$ dimension
$\mathbf{K}_c$	variation in modal stiffness matrix due to crack of $N \times N$ dimension
L_b	beam length
L_1	step location on the beam
L_c	crack location
m_b	mass per unit length of the beam
$\mathbf{M}$	modal mass matrix for intact beam of $N \times N$ dimension
M_b	beam total mass
M_d	disk mass
M_{db}	disk to beam mass ratio (M_d/M_b)
N	number of degrees of freedom
q_i	ith generalized coordinate for deflection
$\mathbf{Q}_{dc}^i$	ith mode shape vector for cracked beam with disk of $N \times 1$ dimension
$\mathbf{Q}_d^i$	ith mode shape vector for intact beam with disk of $N \times 1$ dimension
R_d	disk radius of gyration about Z-axis
R_{db}	non-dimensional parameter R_d/L_b
t^*	reference time $= \sqrt{3\rho L^4/EH_2^2}$
T, U	beam kinetic and strain energy, respectively
V_b	lateral beam deflection
β_d^i	ith non-dimensional natural frequency of intact beam with disk
β_{dc}^i	ith non-dimensional natural frequency of cracked beam with disk
ϕ_i	ith mode shape for lateral deflection
κ_c	crack equivalent stiffness
θ_Z	beam cross-section angel of rotation due to bending
Θ_c	dimensionless crack equivalent flexibility
τ	t/t^*
ξ	x/L_b
ξ_c	L_c/L_b
ξ_1	L_1/L_b
$()_b$	quantity related to beam
$()_d$	quantity related to disk
$()_c$	quantity related to crack
$()^{\mathrm{T}}$	transpose form
$(\overset{*}{})$	total derivative with respect to τ
$(\dot{})$	total derivative with respect to t
$()'$	total derivative with respect to ξ
$\Delta(D)$	crack depth distance function
$\Gamma^i(\xi)$	ith mode equivalent crack flexibility
$\sigma(\xi)$	modes distance function

of cracked structures is important. A crack in a structure may be realized from the local discrepancy in structure stiffness affecting the global dynamic behavior of the structure. Also, a crack may manifest its presence in a beam-like structure through the changes in the natural frequencies and mode shapes of the system. These indicators may also be used to measure the extent of the damage and to determine its location.

Several researchers showed interest in developing algorithms to detect cracks in beams. The motivation for this interest is that the identification of cracks in a beam furnishes an important point of reference to test the precision of identification techniques; also, many mechanical systems have a dynamic behavior similar to a single beam, like shafts, blades and robot arm.

The fact that a crack or a local defect affects the dynamic response of a structural member is known long time ago. Numerous attempts aimed to quantifying the local defects are reported in the literature. The effect of a notch on the structure flexibility is simulated by a local flexibility, a local bending moment or a reduced cross section, with magnitudes that were estimated by experimentation or by the use of fracture mechanics methods. In most studies, researchers utilize the changes in the system's dynamic behavior as a diagnostic tool for damage detection.

A comprehensive literature survey of the analytical, numerical and experimental investigations on the detection of a structural flaw based on the changes in dynamic characteristics can be found in Dimarogonas [1]. Chondros and Dimarogonas [2] modeled the presence of a crack and the corresponding reduction of flexural stiffness by means of a linear massless rotational spring, whose stiffness is related to crack depth. Chondros et al. [3] developed a theory for modeling the lateral vibration of cracked Euler–Bernoulli continuous beams with single or double-edge open cracks. They derived the governing differential equation of motion and the corresponding boundary conditions of a cracked beam assuming a one-dimensional continuum. By describing a displacement field near the crack, fractural mechanics was used to model the crack as a continuous flexibility. Also, Chondros et al. [4] detected crack by using a continuous cracked beam vibration theory for prediction of changes in the transverse vibration of a simply supported beam with a breathing crack. He et al. [5] proposed a genetic algorithm based method for shaft crack detection. Dharmaraju et al. [6] developed a general identification algorithm to estimate the crack flexibility coefficients and the crack depth based on the forced response information of the beam. They used an Euler–Bernoulli beam element in the FE modeling, and the crack has been modeled by a local compliance matrix, with four degrees of freedom. Zheng and Kessissoglou [7] used a finite element method (FEM) to obtain the natural frequencies and mode shapes of a cracked beam. They obtained the total structure flexibility matrix by adding the crack flexibility to the flexibility matrix of the intact beam element as an overall additional flexibility matrix instead of adding it as local flexibility matrix; using this derivation, they were able to predict the natural frequencies more accurately. Sekhar [8] proposed a method for on-line identification of a rotor with dual cracks. The FEM is used to model the rotor, and the cracks are introduced as additional local flexibility to the system flexibility. Ruotolo et al. [9] investigated the forced harmonic response of a cracked cantilever beam. Their study was performed using a FE model that is called the closing crack model. Undamaged parts of the beam were modeled using an Euler-type FE having two degrees of freedom: transverse displacement and rotation at each node. Both fully opened and fully closed cracks were used to represent the damaged element. Chen and Jeng [10] exploited a FE model to investigate the dynamical behavior of pre-twist rotating blades with a single edge crack. They investigated the effect of crack position and crack depth on the natural frequencies of the blade. Yang et al. [11] studied the influence of cracks on the vibration of a beam by using an energy-based numerical model. They used Galerkin's method to determine beam modes and frequencies. Dilena and Morassi [12] identified cracks by utilizing the shifts in beam natural frequencies and anti-resonant frequencies due to a crack. The theoretical results are verified by comparison with the dynamic measurements that performed on cracked steel beams with free–free boundary conditions. Gounaris and Papadopoulos [13] proposed a new technique for crack detection in a beam. They studied a model that has a transverse surface crack that was assumed to be always opened. The technique is based on the fact that the eigenmodes of any cracked structure are different from those of an un-cracked one. Their concept was to link the mode shape differences with the crack position and depth. The correlated differences were chosen to be: (a) the amplitude ratio, measured at two positions, and (b) the position of the node of the vibrating mode. Masoud et al. [14] suggested a mathematical model to study the effect of crack depth on the transverse vibration characteristics of a pre-stressed fixed–fixed cracked beam. They studied the effect of interaction between the crack depth and axial load on the beam natural frequencies. An experimental verification was carried that verified the obtained theoretical results. Chati et al. [15] studied the dynamic characteristics of a cantilever beam having a transverse edge crack by using modal analysis. The nonlinearity induced from the crack opening and closing was modeled as a piecewise linear system utilizing the idea of bilinear frequencies. The FEM was used to obtain the natural frequencies in each linear region. Also, a perturbation method was used to obtain the non-linear normal modes of vibration and the related period of motion. Hasan [16] used a perturbation method to evaluate the first order perturbation of the eigenfrequencies of a beam on an elastic foundation. The local flexibility introduced by the crack in the cracked section was represented by a massless torsional spring whose stiffness dependeds on the severity of the crack. He found that the magnitude of change in the eigenfrequenies is a function of the severity and the location of the crack. Sunder et al. [17] used the weak non-linear character of a cracked vibrating beam to determine the crack location and depth. Chen and Chen [18] investigated the stability of a rotating cracked shaft subjected to an axial compressive end force. They investigated the effect of existing opened cracks on the whirling speeds of the shaft. They showed that two principal instability regions of different types appear, namely divergence and flutter, when the shaft is subjected to an increasing end load.

Tsai and Wang [19] studied vibration of a rotor with multiple cracks. More recently, Chondros [20] used the variational principle to derive the governing eqution of motion for the torsional vibration of a cylindrical shaft with circumferential crack. He used fracture mechanics to find the displacement field in the vicinity of the crack, which is used to model the crack as continuous flexibility.

Most of the crack identification techniques cited in the previous literature are applied to a uniform cross section beam like structure, without including the effects of beam rotary inertia and any lumped attachments like a disk carried by the beam. Including the effects of beam rotary inertia and/or lumped attachments requires employing techniques that use complicated and lengthy modeling procedures as FE in which, a cracked beam element has been developed to simulate the crack, or a very fine mesh in the vicinity of the crack is used in the case of three-dimensional FEA. Also the disk in these works was modeled as concentrated mass along the beam axis. Furthermore, varying the crack location in FEA is difficult and lengthy task since it requires rebuilding of the FE model for each new crack location. In addition, most of the previous works treated the crack as an additional local flexibility that introduced to the global flexibility of the intact beam to obtain the total cracked beam flexibility matrix. Most of crack identification techniques utilize the global change in the structure dynamic characteristics due to crack to identify it, consequently introducing the crack as local flexibility may lead to inaccurate modeling of the cracked beam [7]. Also, if a disk is attached to the structure, an additional alteration is introduced to its global dynamic characteristics due to its translational and rotary inertia. As the modal methods exploit the global changes in the dynamic characteristics of a structure to detect crack, the modification resulting from an attached disk will interfere with that resulting from crack. Therefore, if the variation in the global system dynamic characteristics (natural frequencies and mode shapes of the system) is used to identify cracks precisely, the interaction effect between the attached disk and the crack should be taken into consideration. In addition the crack flexibility should be introduced as global effect in the system flexibility.

The present work proposes a simple crack identification technique based on a suggested mathematical model to identify crack position and depth in a stepped cantilever beam carrying a rigid disk at its tip. The identification technique utilizes the difference in the first three natural frequencies between a cracked and intact beam to identify the crack location and depth. It has many advantages because it based on a mathematical model that account for the interaction between the effects of crack, beam rotary inertia and disk inertia on the dynamic characteristics of the beam. The governing equations of motion for the stepped beam carrying a rigid disk are derived using the assumed mode method combined with Lagrange's equation. Using this method to model the beam under consideration and adopting a crack model [21] to represent its flexibility lead to a simple mathematical model that introduce the crack and the disk inertia as global quantity. Consequently their effects on the system dynamic characteristics will appear as global one. This appearance matches the real case in which the effects of the crack and the disk inertia are observed through the global modification of the system dynamic characteristics (natural frequencies and mode shapes). The mode shapes for two uniform beams connected by a massless torsional spring (simulating the cracked beam) are used as trial functions in the assumed mode method [14]. The proposed mathematical model is verified using 3-D FEA with very fine mesh in the vicinity of the crack, where the commercial FE package ANSYS (version 8) is used in the simulation. The effect of crack depth and location on the system's natural frequencies is investigated. To demonstrate the reliability and the accuracy of the proposed crack identification technique, FE results are used to represent measured data; these data are introduced into the crack identification technique to retrieve the crack depth and location.

2. Mathematical modeling

The lateral vibration of a fixed-free stepped beam with symmetrical double-sided crack carrying a rigid disk at its tip is modeled (Fig. 1a). The beam is assumed to have uniform mass density, modulus of elasticity, and two dissimilar uniform rectangular cross sections. The disk is modeled as a concentrated mass, with rotary moment of inertia, attached to the beam tip. Also the shaft cross section rotary inertia is included in the model. A massless torsional spring whose stiffness depends on the severity of the crack is used as crack model. Using this crack modeling method combined with the assumed mode method, the crack effect can be introduced to the system as global additional structural flexibility.

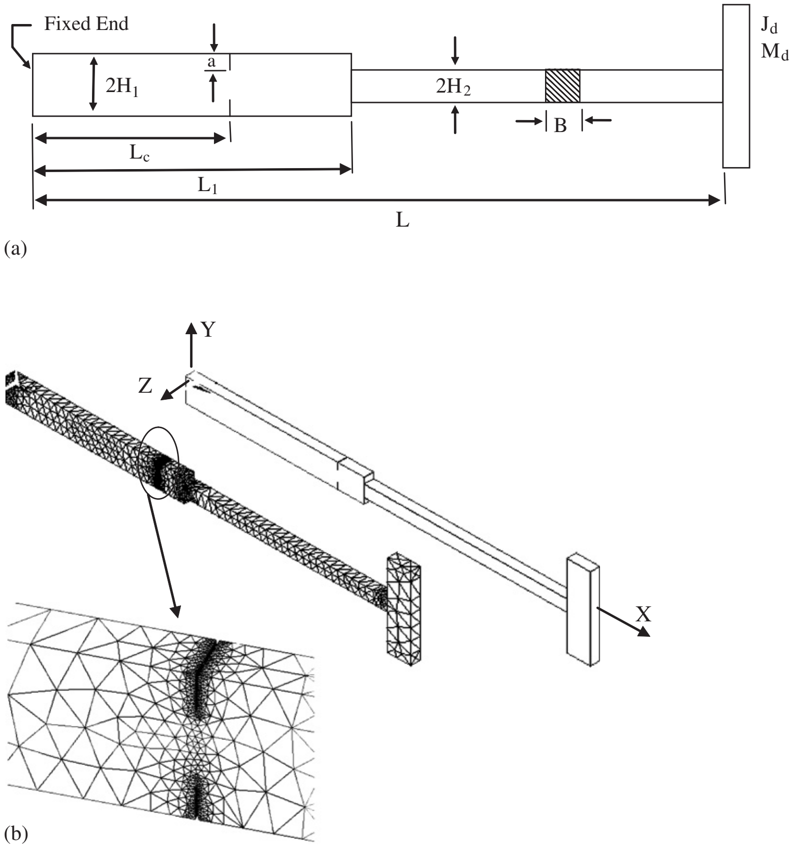

Fig. 1. (a) Schematic diagram for cracked stepped beam carrying a rigid disk and (b) solid model used in finite element and the mish layout for the beam.

The beam centerline is assumed to have only lateral deformation in the Y direction equal to $V_b(x, t)$. Due to this lateral deformation, the beam cross section has a rigid body rotation about the Z-axis, $\theta_Z = \partial V_b(x,t)/\partial x$. The beam deformation causes disk rigid body translation and rotation equal to $V_b(L_b, t)$ and $\theta_d = \partial V_b(L_b,t)/\partial x$, respectively. As a result of the above motions the system kinetic (T) and strain (U) energies will be:

$$T = \frac{1}{2}\int_0^{L_b} m_b(x)\left[\frac{\partial V_b(x,t)}{\partial t}\right]^2 \mathrm{d}x + \frac{1}{2}\int_0^{L_b} J(x)\left[\frac{\partial^2 V_b(x,t)}{\partial t \partial x}\right]^2 \mathrm{d}x + \frac{1}{2}M_d\left[\frac{\partial V_b(L_b,t)}{\partial t}\right]^2 + J_d\left[\frac{\partial^2 V_b(L_b,t)}{\partial t \partial x}\right]^2, \quad (1)$$

$$U = \frac{1}{2}\int_0^{L_b} EI(x)\left[\frac{\partial^2 V_b(x,t)}{\partial^2 x}\right]^2 \mathrm{d}x + \frac{1}{2}\frac{(EI_c)^2}{\kappa_c}\left[\frac{\partial^2 V_b(L_c,t)}{\partial^2 x}\right]^2, \quad (2)$$

where $1/\kappa_c$ is rotational spring flexibility that used to model a double-sided crack [21]

$$\frac{1}{\kappa_c} = \frac{9\pi D^2}{BH_c^2 E}(0.5033 - 0.9022D + 3.412D^2 - 3.181D^3 + 5.793D^4),$$

where B is beam width (measured in the Z direction), D crack depth ratio (crack depth to half beam height at crack location), H_c half beam height at crack location and E is the modulus of elasticity of the material. The above equivalent crack modeling has a significant accuracy for crack depth ratio less than 0.5. This was shown by two different manners; experimentally by Masoud [14] and using FEA by Haisty [21]. As far as the assume mode method is concerned, the beam centerline deflection $V_b(x, t)$ is expressed as

$$V_b(x,t) = \sum_{n=1}^{N} \phi_n(x) q_n(t), \tag{3}$$

where $q_n(t)$ is the nth generalized coordinate and $\phi_n(x)$ is the nth bending mode shape for constant cross section cracked beam [14]. Substituting the centerline deflection, Eq. (3) into the kinetic and strain energies Eqs. (1) and (2) then applying the Lagrange's equation

$$\frac{\mathrm{d}}{\mathrm{d}t}\left(\frac{\partial T}{\partial \dot{q}_i}\right) - \frac{\partial T}{\partial q_i} + \frac{\partial U}{\partial q_i} = 0 \tag{4}$$

lead to the equations of motion for the system. The non-dimensional form of these equations for any generalized coordinate q_m is

$$\begin{aligned}
&\Bigg[[M_{db}((H_{12}-1)\xi_1+1)(\phi_m(1)\phi_n(1)+R_{db}^2\phi_m'(1)\phi_n'(1)) + H_{12}\int_0^{\xi_1}\phi_m(\xi)\phi_n(\xi)\,\mathrm{d}\xi \\
&+\int_{\xi_1}^{1}\phi_m(\xi)\phi_n(\xi)\mathrm{d}\xi + \frac{H_{2L}^2}{3}\left(H_{12}^3\int_0^{\xi_1}\phi_m'(\xi)\phi_n'(\xi)\mathrm{d}\xi + \int_{\xi_1}^{1}\phi_m'(\xi)\phi_n'(\xi)\mathrm{d}\xi\right)\Bigg]\overset{**}{q_n} \\
&+\left[H_{12}^3\int_0^{\xi_1}\phi_m''(\xi)\phi_n''(\xi)\mathrm{d}\xi + \int_{\xi_1}^{1}\phi_m''(\xi)\phi_n''(\xi)\mathrm{d}\xi + H_{c2}^3\Theta_c\phi_m''(\xi_c)\phi_n''(\xi_c)\right]q_n = 0, \\
&n = 1,2,\ldots,N, \quad m = 1,2,\ldots,N,
\end{aligned} \tag{5}$$

where (Θ_c) is the non-dimensional flexibility of the symmetric double-sided crack and given by

$$\Theta_c = 6\pi D^2 \frac{H_c}{L_b}(0.5033 - 0.9022D + 3.412D^2 - 3.181D^3 + 5.793D^4).$$

If a simple harmonic motion is assumed for beam deflection, the non-dimensional differential equation is represented in the following eigenvalue problem format:

$$[-(\beta_{dc}^i)^2\mathbf{M} + \mathbf{K} + \Theta_c\mathbf{K}_c]\mathbf{Q}_{dc}^i = \mathbf{0}, \tag{6}$$

where the elements of matrix $\mathbf{K}_c$ are the second derivative of the trial functions evaluated at crack location only, and β_{dc}^i is the ith non-dimensional natural frequency of the system. The above equation is reduced to represent the lateral vibration of intact beam carrying rigid disk, if the crack flexibility Θ_c is set to zero:

$$[-(\beta_d^i)^2\mathbf{M} + \mathbf{K}]\mathbf{Q}_d^i = \mathbf{0}. \tag{7}$$

After mathematical manipulation for Eqs. (6) and (7), the crack flexibility can be obtained in terms of the intact and cracked system dynamic characteristics as

$$\begin{aligned}
&\Theta_c = \Gamma^i(\xi), \\
&\Gamma^i(\xi) = \frac{(\beta_{dc}^i)^2 - (\beta_d^i)^2}{(\beta_d^i)^2} \times \frac{\mathbf{Q}_d^{i\mathrm{T}}\mathbf{K}\mathbf{Q}_d^i}{\mathbf{Q}_{dc}^{i\mathrm{T}}\mathbf{K_c}\mathbf{Q}_{dc}^i}.
\end{aligned} \tag{8}$$

$\Gamma^i(\xi)$ is named as ith mode equivalent crack flexibility. The value of Θ_c depends on the crack depth only. Consequently, for a specific system its value is constant for all modes of vibration. Thus, crack location can be predicted by plotting the value of $\Gamma^i(\xi)$ versus location on beam span (ξ) for the first three modes. Theoretically these modes will intersect at a single point, which is the crack location. However, in reality, the modes frequency values of β_{dc} and β_d are found experimentally with some measuring error. Therefore $\Gamma^i(\xi)$ curves will not intersect at a single point; instead, they will intersect within a small region. To simplify the crack position search, a modes distance function $\sigma(\xi)$ is defined as

$$\sigma(\xi) = \frac{1}{\mathrm{NM}}\left[\left|\frac{\Gamma^1(\xi) - \Gamma^{\mathrm{NM}}(\xi)}{\Gamma^1(\xi)}\right| + \sum_{i=1}^{\mathrm{NM}-1}\left|\frac{\Gamma^i(\xi) - \Gamma^{i+1}(\xi)}{\Gamma^1(\xi)}\right|\right], \tag{9}$$

where NM is the number of measured system natural frequencies, which is equal to three in this work. Theoretically, this function is equal to zero at the crack location, but in reality, this function has a minimum value at crack location.

After detecting the crack location, the crack depth is identified by substituting the detected crack location into Eq. (6) to calculate the theoretical frequency change in the first three modes of vibration due to the crack for different crack depths. Ideally, at the estimated crack depth all theoretical frequencies shifts should perfectly match with the experimental ones. However, practically this is not the case and each frequency shift will individually match with the corresponding experimental one for a certain crack depth. Therefore, to estimate crack depth accurately, a crack depth distance function $\Delta(D)$ is defined as

$$\Delta(D) = \frac{1}{\mathrm{NM}}\sum_{i=1}^{\mathrm{NM}}\left|\left(\frac{\beta^i_{dc} - \beta^i_d}{\beta^i_d}\right)_{\text{measured}} - \left(\frac{\beta^i_{dc} - \beta^i_d}{\beta^i_d}\right)_{\text{theory}}\right|. \tag{10}$$

If this function is plotted versus crack depth, its value will be zero at the estimated crack depth in the ideal situation. However, in reality this function has its minimum value in the vicinity of the estimated crack depth.

Two methods are usually used to verify the reliability of the proposed mathematical model: the first one is experimental while the second is the FEA. In this work, FEA is considered as method of verification, because it provides a simple and inexpensive way to generate as much checked points as desired. Three-dimensional FEA is carried out using the commercial software ANSYS 8.0 to verify the results obtained from the proposed mathematical model. In FEA, 10-node tetrahedral element type was used to model clamped-free stepped beam carrying a rigid disk; the crack is represented by sharp V-notch. A non-uniform mesh with very fine mesh in the vicinity of the crack is used in FE modeling (Fig. 1b). Also, convergence test to the first four natural frequencies of the beam was applied to insure high precision results.

3. Results and discussion

A mathematical model to simulate lateral vibration of a stepped cantilever cracked beam carrying a rigid disk at its tip is proposed utilizing the assumed mode method. The crack is modeled as equivalent massless rotational spring with flexibility derived from fracture mechanics concepts. This mathematical model is used as a base for crack identification algorithm. The number of trial functions used in the assumed mode method is taken to be $N = 11$ to warrant high precision in calculating the first three natural frequencies of the system. These trial functions are found by solving the eigenvalue problem of two equal cross section beams connected by massless torsional spring at the crack position [14]. The effects of crack depth and location on the first three natural frequencies of the system are investigated. The results obtained from the proposed mathematical model are compared with the results obtained by using FEA. In FEA a steel beam ($E = 207\,\mathrm{GPa}$, $G = 79\,\mathrm{GPa}$, $\rho = 7700\,\mathrm{Kg/m^3}$, $\upsilon = 0.3$) with the following dimensions in millimeters: $B = 8$, $H_1 = 10$, $H_2 = 5$, $L_1 = 300$, $L = 650$ is used (Fig. 1a). The disk dimensions in millimeters are: height $= 70$, thickness $= 20$, width $= 8$ and its material properties are ($E = 2070\,\mathrm{GPa}$, $G = 790\,\mathrm{GPa}$, $\rho = 52250\,\mathrm{Kg/m^3}$, $\upsilon = 0.3$). Using the aforementioned material properties will lead to a rigid disk (relative to the beam) having a mass equal to the beam mass. For certain crack depth and location the first three frequencies of cracked and intact beams are found using FEA. These values are considered as experimentally measured data and are substituted into the proposed identification technique to retrieve the crack location and its depth.

The effect of the attached disk and the crack location on the first three natural frequencies of the system is presented in Figs. 2–4 for different crack depth ratios. Fig. 2 shows the variation in the first natural frequency change ratio due to crack versus wide range of crack locations and depths. The figure indicates that decreasing the distance between the crack and the beam tip reduces the frequency change ratio. This ratio exhibits big reduction jump when the crack crosses the step section. In addition, the figure illustrates that attaching a disk

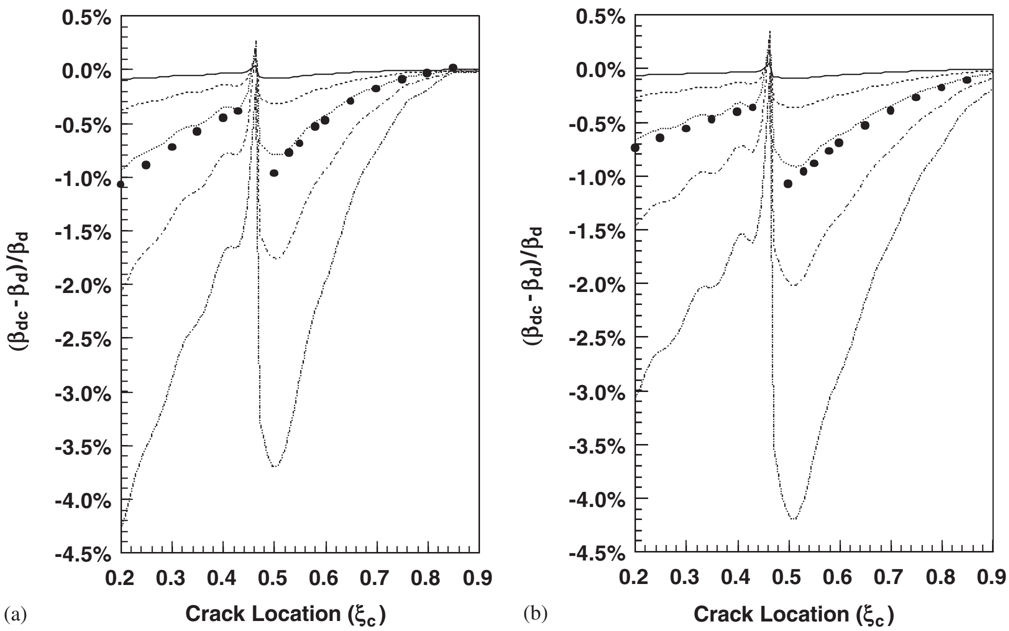

Fig. 2. First natural frequency change ratio due to crack versus crack location. (a) Disk mass $M_d = 0.0$ and (b) disk mass $M_d = 1.0$; $R_{db} = 0.03581$. Crack depth ratio (D): FE: ●, 0.3; theoretical; ———, 0.1; — — — —, 0.2; ············, 0.3; — · —, 0.4; — · · —, 0.5.

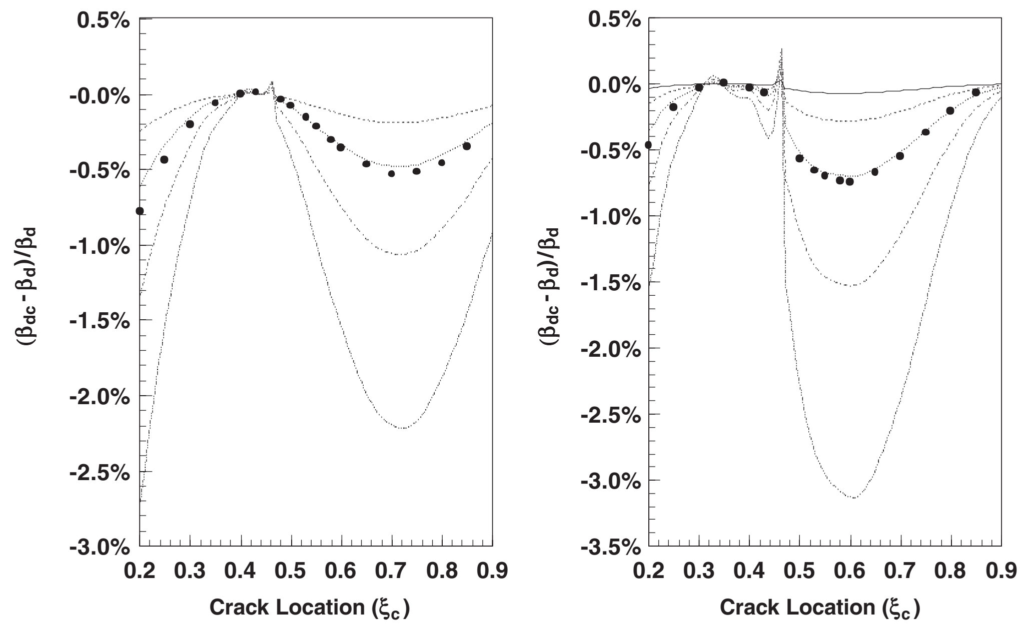

Fig. 3. As Fig. 2 but for second natural frequency.

to the beam decreases the above change by a noticeable amount if the crack position is on the thick side of the beam. On the contrary, if the crack position is on the thin side of the beam the above change ratio is slightly increased. These results are observed for all crack depths. The second natural frequency change

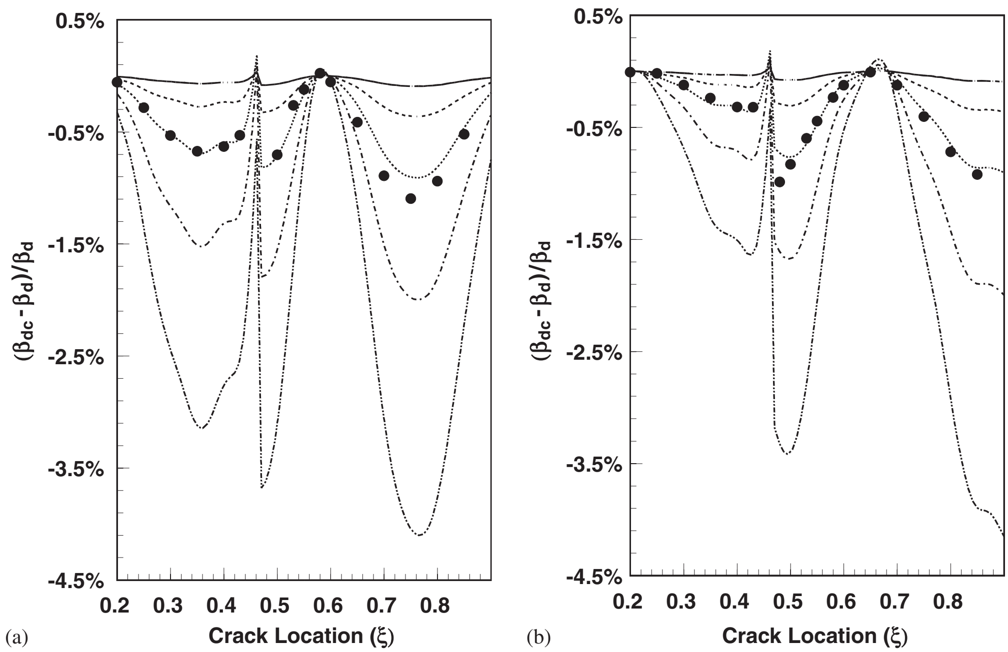

Fig. 4. As Fig. 3 but for third natural frequency.

ratio versus crack location is presented in Fig. 3 for different crack depth values. This figure reveals that decreasing the distance between the crack and the beam tip decreases the above ratio in some regions and increases it in some others. Attaching the disk to the beam tip increases this ratio when the crack is located on the thick side, away from the step, but when it is located close to the step this ratio decreases. If the crack is located in the thin side, the disk causes reduction of the above ratio by slight amount. These results are observed for all crack depth values. The third natural frequency change ratio versus crack location is shown in Fig. 4. This figure shows that the above ratio has high fluctuation versus crack location.

In all previous figures, the results obtained from the proposed mathematical model show sound agreement with the FEA results, except in a very narrow region at the step location where there is a little deviation between the two groups of results. This is related to the sharp change in the beam geometry, which may lead to numerical computational error in the proposed mathematical model when the crack is close to the step. Also the mathematical model does not account for the stress concentration due to the step in the beam in addition to neglecting the interaction between the above stress and the one created from the crack. However, the fluctuations observed in the model results are also traced by those of FEA. These fluctuations are explained by the fact that the influence of crack is altered by the mode curvature as well as by the closeness of the crack to beam nodes. For the first three natural frequencies Fig. 5 shows the effect of crack depth on the frequency change ratio for crack located on the thick side ($\xi_c = 0.4$) and on the thin side ($\xi_c = 0.75$), for beam with and without a disk. It can be seen that increasing the crack depth will increase the above ratio for a beam with or without a disk, and for both crack locations; on the contrary, attaching the disk to the beam reduces the above ratio for both crack locations. The results obtained from the model are traced also by FEA approach. An interesting phenomenon is noticed for the crack located at $\xi_c = 0.4$, whereby adding a disk to the beam caused the changes in the first and the third natural frequencies ratios close to each other. This is due to having the beam curvature for the first and the third modes close to each other at this location when the disk is introduced. This observation demonstrates that in order to use the variations in system frequencies to identify crack, the interaction between the effects of the crack and the disk inertia on the dynamic characteristics of the beam should be included in the analysis.

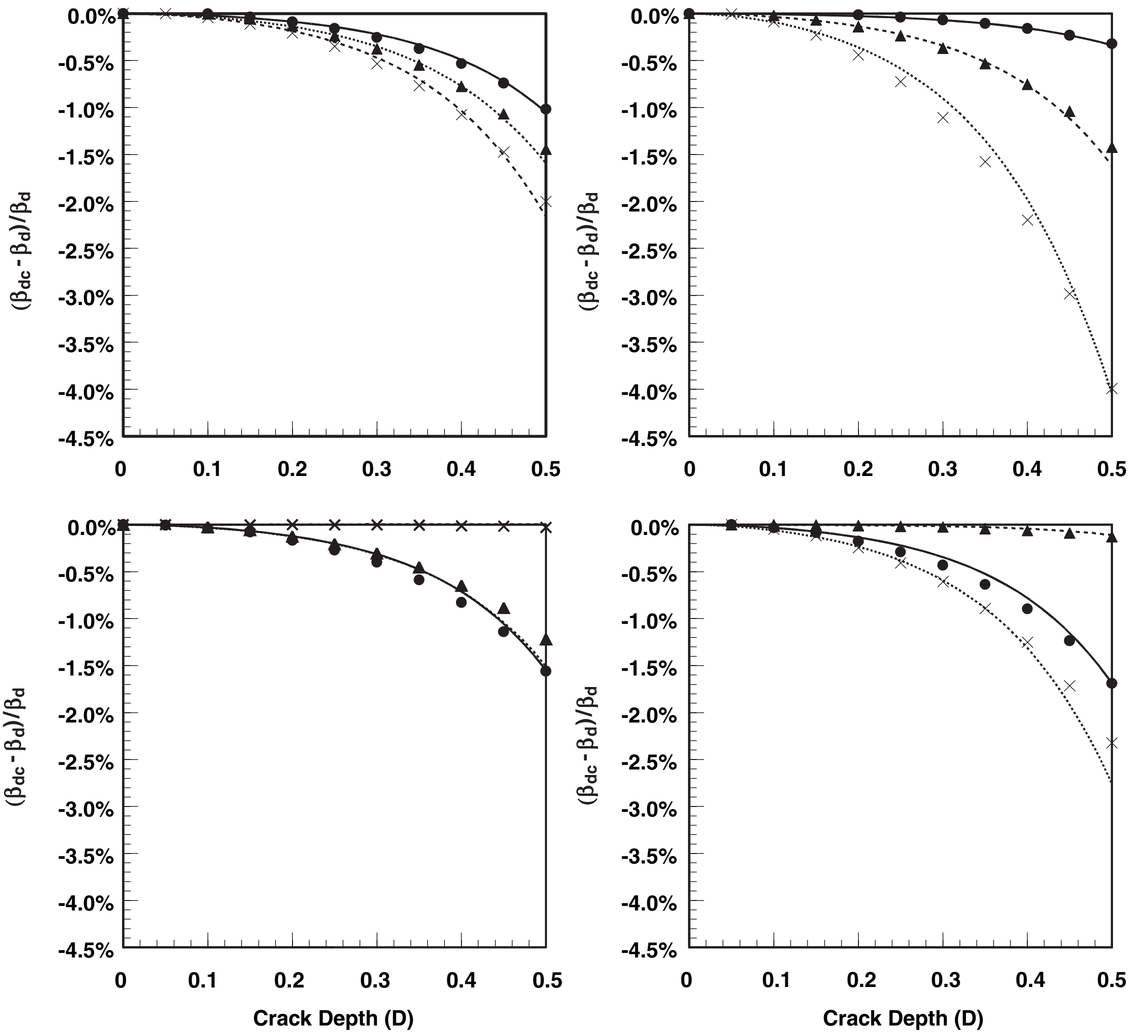

Fig. 5. The first three natural frequencies change ratios versus crack depth. $R_{db} = 0.03581$, (a) disk mass $M_d = 0$ crack location $\xi_c = 0.75$, (b) $M_d = 1$ $\xi_c = 0.75$, (c) $M_d = 0$ $\xi_c = 0.4$, (d) $M_d = 1$ $\xi_c = 0.4$. FE: ●, 1st; ×, 2nd; ▲, 3rd. Theoretical: ——, 1st; — — — —, 2nd; ············, 3rd.

With the confidence gained by comparing the results obtained from the proposed mathematical model with that of the FEA, the FEA values for the first three frequencies for cracked and intact beams with attached disk are substituted into the proposed identification technique to retrieve the crack that is introduced into the FE model. Figs. 6 and 7 show different cases of crack location prediction, where the modal equivalent crack flexibility ($\Gamma^i(\xi)$) and the modes distance function ($\sigma(\xi)$) are plotted versus beam span location. The crack location can be estimated from the $\sigma(\xi)$ curve where the lower sharp edges are pointing to a potential crack position. The results reported in Fig. 6 show that the $\sigma(\xi)$ curve has only a single lower sharp edge pointing to the crack location. This single indicator is found in the majority of the test cases, leading to unique prediction of crack location. On the other hand, for few cases, the $\sigma(\xi)$ function predicts multiple crack locations as shown in Fig. 7. This multiple prediction can be reduced by cross-referencing the sharp edges of the $\sigma(\xi)$ function with the $\Gamma^i(\xi)$ functions. Since the values from the $\Gamma^i(\xi)$ curves should be equal at actual crack location, thus relating the sharp edge points in the $\sigma(\xi)$ curve to the $\Gamma^i(\xi)$ curves intersection leads to a potential actual crack location; this reduces the multiple prediction points using $\sigma(\xi)$ curve to one or two locations only.

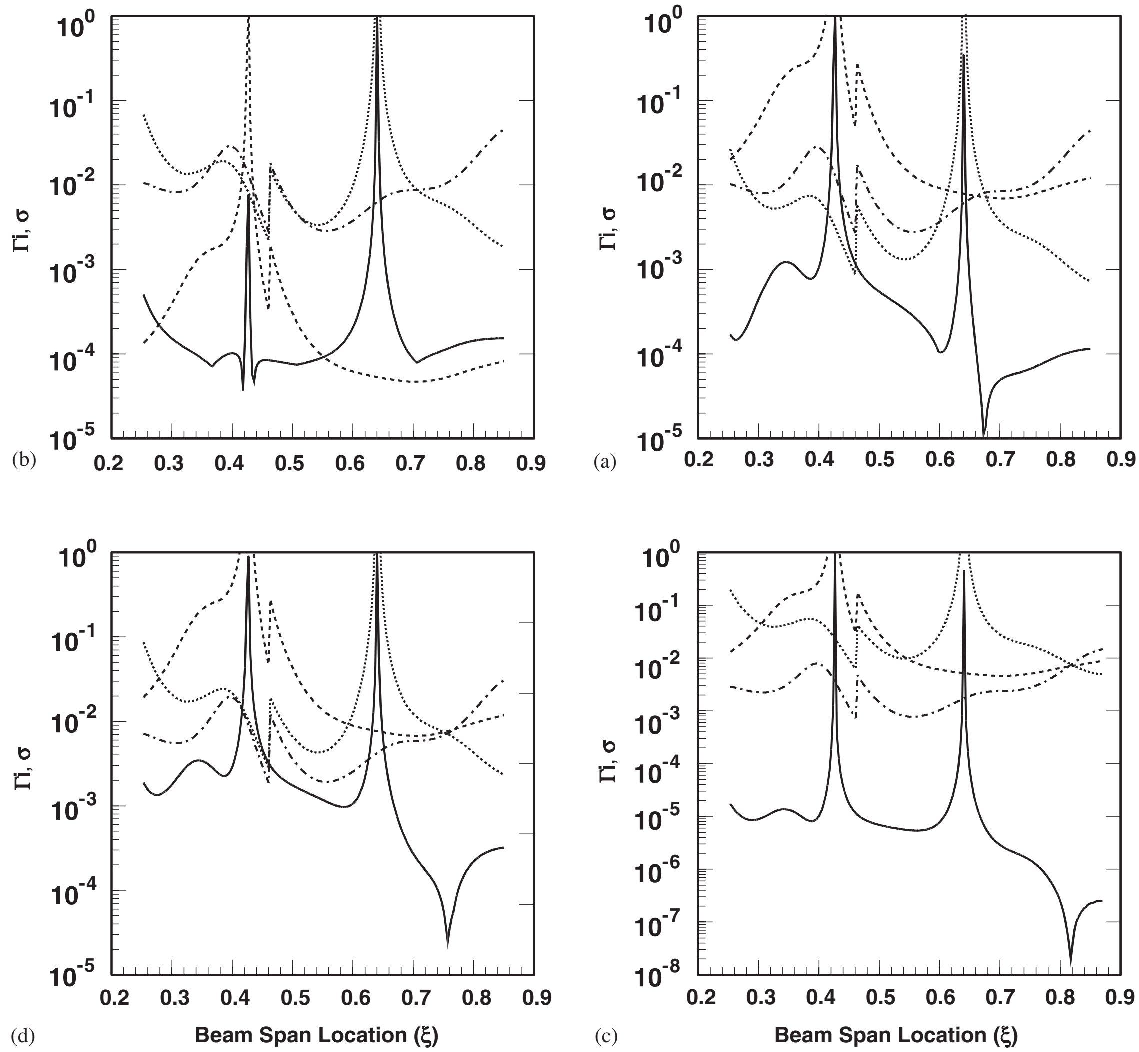

Fig. 6. Mode equivalent crack flexibility $\Gamma^i(\xi)$ and Modes distance function $\sigma(\xi)$ versus beam span location (ξ) $M_d = 1.0$; $R_{db} = 0.03581$. ———, $\sigma(\xi)$; — · —, Γ^1; — — — —, Γ^2; ············, Γ^3. (a) $\xi_c = 0.7$, (b) $\xi_c = 0.4$, (c) $\xi_c = 0.85$ and (d) $\xi_c = 0.75$.

After anticipating the crack location, the crack depth distance function $\Delta(D)$ is plotted versus crack depth. The first three theoretical frequencies change ratio are found by substituting the predicted crack location into the proposed mathematical model. The measured frequency change ratios are taken to be the FEA values. Fig. 8 presents the $\Delta(D)$ function versus crack depth in terms of different crack positions and for an actual crack depth ratio of 0.3. The curve has its minimum value at a potential crack depth value, and it can be seen from the figure that the minimum curves values are around the actual crack depth.

Table 1 shows the actual crack location and depth values versus the estimated ones found from Figs. 6–8, also additional cases that have distinctive prediction results are reported in this table. It can be seen that in few cases the method predicts multiple crack locations; however, one of these is in the neighborhood of the actual crack location. Using the predicted crack location closer to the actual one to find the crack depth, a single crack depth value is estimated; also, this value is found to be very close to the actual crack depth. The percentage error in predicting crack location or depth varies between 1% and 11%.

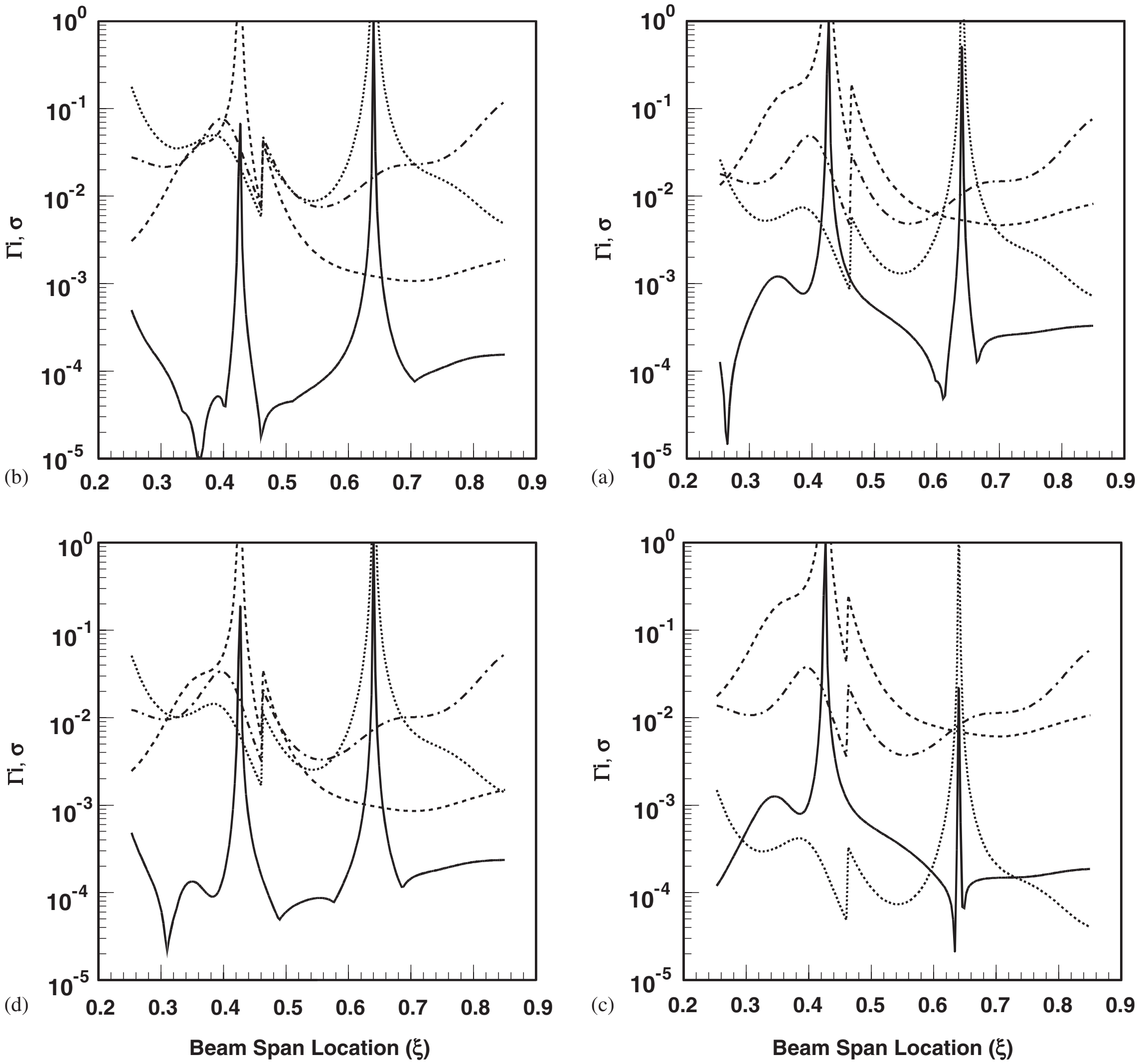

Fig. 7. As Fig. 6 but for (a) $\xi_c = 0.6$, (b) $\xi_c = 0.5$, (c) $\xi_c = 0.65$ and (d) $\xi_c = 0.35$.

4. Conclusion

This research proposed a simple technique based on mathematical model to identify crack location and depth in a stepped cracked cantilever beam carrying a rigid disk. Using the assumed mode method combined with Lagrange's equation, a simple mathematical model describing the lateral vibration of the beam is derived. In that formulation the crack is modeled as a massless spring. Its flexibility is added to the global intact beam flexibility matrix as global flexibility. The mathematical model accounts for the beam rotary inertia as well as the interaction between the crack and the disk inertia. The results obtained from the proposed model were traced by similar results obtained from FEA. The proposed crack identification algorithm has the capability to predict the crack location in addition to its depth by furnishing simple functions: $\sigma(\xi)$ (modes distance function) to estimate crack location, as well as $\Delta(D)$ function (crack depth distance function) to estimate crack depth. These two functions utilize the derived mathematical model and the measured variation in the first three natural frequencies due to crack for its identification. These two functions enable estimating the crack depth and its location with an accuracy ranging from 1% to 11%.

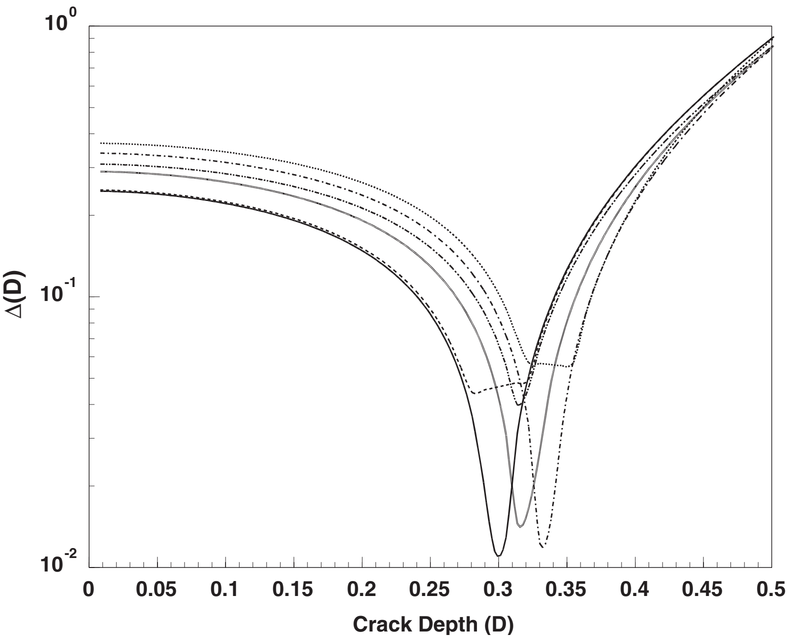

Fig. 8. Crack depth distance function $\Delta(D)$ versus crack depth ratio (D). Actual crack depth ratio $D = 0.3$. Crack depth location ξ_c: ——, 0.3; – – – –, 0.4; ··········, 0.5; — · —, 0.6; — · · —, 0.7; ═══, 0.8.

Table 1
Crack identification results using FE data

Crack location (ξ_c)			Crack depth (D)		
Actual	Estimated	Error %	Actual	Estimated (using estimated ξ_c)	Error %
0.30	0.277	7.7	0.3	0.297	1.0
0.35	0.310	11.4	0.3	0.305	1.7
0.40	0.418	4.5	0.3	0.281	6.3
0.50	0.460	8.0	0.3	0.347	15.7
0.55	0.560	1.8	0.3	0.320	6.7
0.60	0.262 or 0.61	129 or 1.7	0.3	0.320	6.7
0.65	0.634 or	2.5 or	0.3	0.318	6.0
	0.647	0.5			
0.70	0.673	3.9	0.3	0.308	2.7
0.75	0.757	0.9	0.3	0.317	5.7
0.80	0.793	0.9	0.3	0.309	3.0
0.85	0.818	3.8	0.3	0.317	5.7
0.40	0.415	3.75	0.5	0.47	6.0
0.40	0.415	3.75	0.4	0.39	2.5
0.40	0.417	4.25	0.3	0.28	6.67
0.40	0.415	3.75	0.2	0.19	5.0
0.40	0.383 or	4.25			
	0.543	35.75	0.1	0.089	11
	0.700	75			
0.75	0.756	0.80	0.5	0.494	1.2
0.75	0.756	0.80	0.4	0.39	2.5
0.75	0.757	0.93	0.3	0.308	2.67
0.75	0.756	0.80	0.2	0.21	5.0
0.75	0.384 or	48.80			
	0.61	18.67	0.1	0.09	10.0
	0.71	5.33			

Acknowledgement

The Author would like to express his thank to Jordan University of Science and technology (Irbid/Jordan) for their financial support for this research.

References

[1] A.D. Dimarogonas, Vibration of cracked structures: a state of the art review, *Engineering Fracture Mechanics* 55 (5) (1996) 831–857.
[2] T.G. Chondros, A.D. Dimarogonas, Identification of cracks in welded joints of complex structures, *Journal of Sound and Vibration* 69 (1980) 531–538.
[3] T.G. Chondros, A.D. Dimarogonas, J. Yao, Continuous cracked beam vibration theory, *Journal of Sound and Vibration* 215 (1998) 35–46.
[4] T.G. Chondros, A.D. Dimarogonas, J. Yao, Vibration of a beam with a breathing crack, *Journal of Sound Vibration* 239 (2001) 57–67.
[5] Y. He, D. Guo, F. Chu, Using genetic algorithms and finite element methods to detect shaft crack rotor-bearing system, *Mathematics and Computers in Simulation* 57 (2001) 95–108.
[6] N. Dharmaraju, R. Tiwari, S. Talukdar, Identification of an open crack model in a beam based on force–response measurements, *Computers and Structures* 82 (2004) 167–179.
[7] D.Y. Zheng, N.J. Kessissoglou, Free vibration analysis of a cracked beam by finite element method, *Journal of Sound and Vibration* 273 (2004) 457–475.
[8] A.S. Sekhar, Model-based identification of two cracks in a rotor system, *Mechanical Systems and Signal Processing* 18 (2004) 977–983.
[9] R. Ruotolo, C. Surace, P. Crespo, D. Storer, Harmonic analysis of the vibrations of a cantilevered beam with a closing crack, *Computers and Structures* 61 (1996) 1057–1074.
[10] L.W. Chen, C.H. Jeng, Vibrational analysis of cracked pre-twisted blades, *Computers and Structures* 46 (1991) 133–140.
[11] X.F. Yang, A.S.J. Swamidas, R. Seshadri, Crack identification in vibrating beams using the energy method, *Journal of Sound and vibration* 244 (2) (2001) 339–357.
[12] M. Dilena, A. Morassi, The use of antiresonances for crack detection in beams, *Journal of Sound and Vibration* 276 (2004) 195–214.
[13] G.D. Gounaris, C.A. Papadopoulos, Analytical and experimental crack identification of beam structures in air or in fluid, *Computers and Structures* 65 (1997) 633–639.
[14] S. Masoud, M.A. Jarrah, M. Al-Maamory, Effect of crack depth on the natural frequency of a pre-stressed fixed beam, *Journal of Sound and Vibration* 214 (1998) 201–212.
[15] M. Chati, R. Rand, S. Mukherjee, Modal analysis of cracked beam, *Journal of Sound and Vibration* 207 (1997) 249–270.
[16] W.M. Hasan, Crack detection from the vibration of the eigenfrequencies of a beam on elastic foundation, *Engineering Fracture Mechanics* 52 (1995) 409–421.
[17] J.N. Sundermeter, R.L. Weaver, On crack identification and characterization in a beam by nonlinear vibration analysis, *Journal of Sound And Vibration* 183 (1995) 857–871.
[18] L.W. Chen, H.W. Chen, Stability analysis of cracked shaft subjected to the end load, *Journal of Sound and Vibration* 188 (1995) 497–513.
[19] T.C. Tsai, Y.Z. Wang, The vibration of multi-crack rotor, *International Journal of Mechanical Sciences* 39 (1997) 1037–1053.
[20] T.G. Chondros, Variational formulation of a rod under torsional vibration for crack identification, *Theoretical and Applied Fracture Mechanics* 44 (2005) 95–104.
[21] B.S. Haisty, W.T. Springer, A general beam element for use in damage assessment of complex structures, *Journal of Vibration, Acoustics, Stress, And Reliability in Design* 110 (1988) 389–394.